Capture cross sections of the acceptor level of iron–boron pairs in *p*-type silicon by injection-level dependent lifetime measurements

Daniel Macdonald[a] and Andrés Cuevas
Center for Sustainable Energy Systems, Department of Engineering, FEIT, The Australian National University, Canberra, ACT 0200, Australia

Jennifer Wong-Leung
Department of Electronic Materials Engineering, Research School of Physical Sciences and Engineering, The Australian National University, Canberra, ACT 0200, Australia

(Received 2 January 2001; accepted for publication 26 March 2001)

Injection-level dependent recombination lifetime measurements of iron-diffused, boron-doped silicon wafers of different resistivities are used to determine the electron and hole capture cross sections of the acceptor level of iron–boron pairs in silicon. The relative populations of iron–boron pairs and interstitial iron were varied by exposing the samples to different levels of illumination prior to lifetime measurements. The components of the effective lifetime due to interstitial iron and iron–boron pairs were then modeled with Shockley–Read–Hall statistics. By forcing the sum of the modeled iron–boron and interstitial iron concentrations to equal the implanted iron dose, in conjunction with the strong dependence of the shape of the lifetime curves on dopant density, the electron and hole capture cross sections of the acceptor level of iron–boron pairs have been determined as $(3\pm2)\times10^{-14}\,\mathrm{cm}^{-2}$ and $(2\pm1)\times10^{-15}\,\mathrm{cm}^{-2}$. © *2001 American Institute of Physics.* [DOI: 10.1063/1.1372156]

I. INTRODUCTION

The recombination properties of FeB pairs in *p*-type silicon are of considerable interest in silicon device technology. The well established difference in the low-injection recombination strengths of interstitial iron (Fe_i) and FeB pairs can be exploited to make very sensitive measurements of the total iron concentration,[1,2] provided the influence of other recombination centers can be discounted. While the fundamental recombination parameters of Fe_i, namely the defect energy level and the electron and hole capture cross sections, are relatively well known,[3] this is not the case for the acceptor level of FeB pairs. The energy level of the latter has been determined by deep-level transient spectroscopy (DLTS) with reasonable accuracy, but measurement of the capture cross sections has been uncertain, with estimates varying by up to two orders of magnitude.[3]

Injection-level dependent recombination lifetime measurements offer an alternative method for determining the electron and hole capture cross sections σ_n and σ_p.[4] If the energy level of the state is known, as is the case for FeB pairs, and if intentionally iron-contaminated samples of significantly different resistivities are prepared, then both cross sections can be determined quite accurately by fitting Shockley–Read–Hall (SRH) recombination curves to measured injection-level dependent lifetime data. As shown in this work, the key to accurate results from this method is to use a large range of dopant densities that generate very different injection-level dependences: in fact often the dependence will change direction as the doping changes. In addition, the dissociation of FeB pairs by strong illumination[1] can be exploited to generate different concentrations of FeB pairs in a sample with a known total iron concentration. This provides further scope for uniquely determining the capture cross sections.

II. FeB PAIRS IN SILICON

There is strong evidence from various studies using DLTS, Hall effect and electron paramagnetic resonance for the existence of two charge states of the FeB pair in silicon, as summarized recently by Istratov *et al.*[3] One state occurs as a donor level at $E_v+0.1\,\mathrm{eV}$, and the other as an acceptor level at $E_c-0.26(\pm0.03)\,\mathrm{eV}$. Brotherton *et al.*[5] argued that the acceptor level must be the dominant recombination center of the two, due to the fact that it is deeper. Standard SRH recombination theory does not establish a mathematical link between energy levels and cross sections, and so it is possible, within this theory, to attribute unreasonably large cross sections to a very shallow level, resulting in stronger recombination behavior than some deeper levels. However, considering that these recombination processes occur through multiple phonon emission, it seems physically reasonable to expect that shallow levels must have very small cross sections for transitions to or from the furthest band edge, due to the prohibitively large number of phonons that are required simultaneously to carry off the energy difference. Consequently, the deeper acceptor level of FeB pairs should provide a much more efficient recombination channel than the donor level. Hayamizu *et al.*[6] showed that the acceptor level does indeed dominate recombination through FeB pairs at room temperature. They performed temperature dependent low-injection lifetime measurements using a microwave-detected photoconductance decay (PCD) method. Their data

[a]Electronic mail: daniel@faceng.anu.edu.au

could only be adequately described by a relatively deep level around 0.29 eV from either band edge, coinciding with previous DLTS measurements of the energy of the FeB acceptor level. Later temperature-dependent lifetime studies further confirmed their results.[7]

Walz *et al.*[8] examined the injection-level dependence of the recombination lifetimes at room temperature of iron-diffused samples for a range of intermediate resistivities, and found that their data could be adequately explained by modeling the combined effect of the acceptor level and the level for interstitial iron. They were able to determine values for the capture cross sections of the acceptor level by fitting SRH curves to the data for the different resistivities. This technique, sometimes referred to as injection-level spectroscopy, can allow more accurate measurement of cross sections than the more commonly used DLTS methods, which require extrapolation of emission rate data to an axis, a process that inherently produces large uncertainties. However, a crucial requirement of the injection-level spectroscopy technique is that samples with widely different dopant densities are used. The important feature of these different resistivities is that the injection-level dependence of the lifetime for a given defect is often markedly different, allowing accurate fitting of SRH curves with a consistent and unique pair of capture cross sections. This method has been used recently to analyze the recombination properties of boron–oxygen complexes in *p*-type Czochralski silicon.[4] The study conducted by Walz *et al.* was restricted to a resistivity range of 1 to 20 Ω cm due to constraints of their measurement method (Elymat). In this work, we study a larger range of resistivities, from 0.3 to 150 Ω cm. This corresponds to 25 times the dopant density range used by Walz *et al.*, a feature which turns out to be very important for uniquely determining the cross sections. Also, we explore a broader range of injection levels for each resistivity, which is of further benefit in accurately calculating the cross sections.

In addition to varying the dopant densities, the dissociation behavior of FeB pairs upon illumination may be used to vary the recombination center densities. By applying various levels of light soaking to the samples before lifetime measurement, different relative populations of FeB pairs and Fe_i are obtained. In our experiments, the total iron concentration is known from the implantation dose, and so the sum of the modeled FeB and Fe_i centers can be forced to equal this value. In this way, a good fit can be achieved for each light-soaking condition and resistivity, with uniquely determined capture cross sections.

III. EXPERIMENTAL METHODS

A. Sample preparation

Sample preparation is critical in an experiment aimed at investigating metals in silicon. Care needs to be taken to ensure that the deliberately introduced impurities occur evenly throughout the bulk of the wafers, as this is essential for accurate injection-level dependent lifetime measurements. Also, the impurities to be studied should not be subject to significant gettering at the surfaces or damaged regions, nor undergo outdiffusion or precipitation in the bulk. In this study, avoiding loss of iron through these processes allows us to determine the bulk iron concentration, after annealing, from a knowledge of the implantation dose. This is important in modeling the lifetime data and allowing the accurate fitting of the SRH parameters.

Boron-doped *p*-type float zone (FZ) silicon samples of four resistivities (0.3, 1, 5, and 150Ω cm) were chosen for this study. The samples were initially etched and cleaned to remove any surface damage and contamination, and then implanted with 70 keV ^{56}Fe to doses of $1\times10^{11}\,cm^{2}$ and $1\times10^{12}\,cm^{-2}$. Annealing was then performed at 900°C for 1 h to distribute the iron uniformly throughout the wafers. FZ silicon was chosen due to its low oxygen and crystallographic defect content, in order to avoid complicating defect reactions during the annealing stage.[4] The solubility limit of interstitial iron[3] at 900°C is about $5\times10^{13}\,cm^{-3}$, and so for a 0.03 cm thick wafer implanted with a dose of $1\times10^{12}\,cm^{-2}$, the resulting bulk concentration would be $3.3\times10^{13}\,cm^{-3}$. This is close to the solubility limit, but as revealed by the results below, does not create significant precipitation. For the $1\times10^{11}\,cm^{-2}$ doses, the solubility limit is comfortably avoided. Some samples were implanted with even higher doses ($1\times10^{13}\,cm^{-2}$), which did result in massive precipitation in the bulk and hence a loss of interstitial iron, as discussed in Sec. V.

During annealing, iron can also precipitate at the Si/SiO_2 interface.[9] To avoid this, the native oxide was removed immediately prior to annealing, and nitrogen gas was used during the anneal to avoid oxide growth. The samples were then cooled rapidly in air to ''freeze'' the iron in the interstitial state. To minimize the possible loss of iron through outdiffusion, samples of the same implanted dose were annealed face-to-face, with the surfaces in contact. Outdiffusion through the rear of the samples should be insignificant due to the initially low surface concentrations there.

A low implantation energy of 70 keV was used to minimize lattice damage, which can act as unwanted gettering sites during the anneal. Such gettering action may result in nonuniform distributions, which can in turn distort the injection-level dependent lifetime measurements. Furthermore, any remaining lattice damage can directly affect the lifetime measurements and also hinder surface passivation. To avoid these potential problems, several microns of silicon were etched from the wafers after annealing to remove the implanted region. Lifetime measurements before and after this etch revealed no discernible change, indicating that residual damage and gettering in the implanted region was negligible.

After annealing and etching, it is necessary to passivate the wafer surfaces to allow reliable bulk lifetime measurements. This was achieved by depositing films of stoichiometric plasma-enhanced chemical vapor deposited silicon nitride.[10] We chose this passivation method because it provides very low surface recombination velocities, and also because the relatively low temperature and short time required for deposition (390°C for 10 min) avoid potential precipitation problems that can occur if higher temperature processes such as oxidation are used. According to the results of Henley *et al.*,[11] the SiN deposition should result in negligible

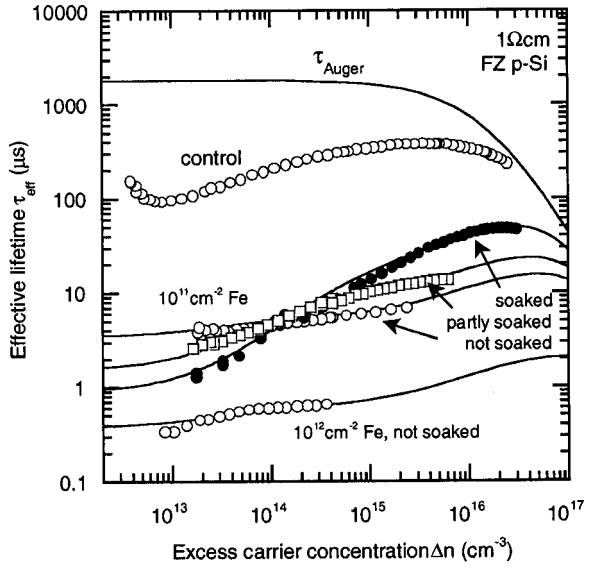

FIG. 1. Lifetime measurements (symbols) and SRH fits (solid lines) for 1 Ω cm samples implanted with iron doses of $1\times10^{11}\,\mathrm{cm}^{-2}$ and $1\times10^{12}\,\mathrm{cm}^{-2}$. For the $1\times10^{11}\,\mathrm{cm}^{-2}$ case, three curves corresponding to different light soaking levels are shown. The concentrations of Fe_i and FeB pairs used to generate the fits are given in Table II, and the recombination parameters in Table I. Also shown are the theoretical Auger limit and data from the nonimplanted control sample.

precipitation for the lighter dose of $1\times10^{11}\,\mathrm{cm}^{-2}$, and only a small proportion (about 10%) for the heavier dose of $1\times10^{12}\,\mathrm{cm}^{-2}$. The effectiveness of the nitride films in passivating the surfaces was verified using control samples, described next. This passivation allows lifetimes of above 1 ms to be observed in high resistivity material.

B. Lifetime measurements

The quasi-steady-state photoconductance (QSSPC) technique[12] was used to measure the injection-level dependence of the effective lifetimes of the iron-diffused samples. This method involves the use of a coil which is inductively coupled to the test wafer, with a circular coil area of about 4 cm^2. The implanted area of our samples was a square of 3 cm×3 cm, large enough to fully cover the measurement region. To ensure that the measured lifetimes reflect the recombination properties of the iron-related states only, and not surface effects or the preimplanted lifetime of the FZ wafers, control samples were included. These were subjected to the same etching, cleaning, annealing, and passivation treatments as the implanted samples. Figure 1 shows injection-level dependent lifetime measurements of the 1 Ω cm wafers. The fact that the effective lifetimes measured on the control samples were almost always an order of magnitude or more greater than the lifetimes of the iron implanted samples means that the measurements on the latter are not significantly affected by surface recombination, nor by the intrinsic bulk lifetime of the FZ wafers. It is in fact this constraint which places a lower limit on the iron dose, as lighter doses would result in surface-affected lifetime measurements. If, however, the dose is too high, and the resultant lifetimes too low, the carrier profiles across the thickness of the samples will become strongly nonuniform (when measuring with white light), and the measured injection level dependence incorrect. It is possible to use an infrared filter to avoid this problem, but the low generation rates of the reduced photon flux do not allow sufficiently high carrier densities to be reached. Consequently, we are restricted to doses around $1\times10^{11}\,\mathrm{cm}^{-2}$ to $1\times10^{12}\,\mathrm{cm}^{-2}$ by considerations of surface recombination, nonuniform carrier profiles, and also by the solubility limit at the chosen annealing temperature.

One further point of interest with respect to photoconductance measurements in general is the observed behavior at very low carrier concentrations. Figure 1 shows that the lifetime abruptly increases below $1\times10^{13}\,\mathrm{cm}^{-3}$ for the control sample. This dependence is not related to SRH recombination through defects, but is a result of minority carrier trapping.[13] These trapping states, which trap and release electrons from the conduction band without directly contributing to recombination, may reside in the bulk or at the SiN/Si interface. In either case, they distort the recombination lifetime measurements in both the control and iron-diffused samples. This trap-affected data does not reflect the recombination lifetime, and must be discarded. This has been done for the iron-doped samples in Fig. 1, and for all subsequent data plotted in this work, although other studies have sometimes failed to recognize this problem and erroneously considered the trap-affected data as SRH recombination lifetimes.[14] The onset of trapping is therefore an effective lower bound on the carrier densities for which reliable recombination lifetime data is available. Surface photovoltage methods are immune to trapping effects, but can only measure lifetimes under very low injection-level conditions and so are not appropriate for injection-level spectroscopy.

IV. SRH STATISTICS

A. Injection-level and dopant density dependence of the lifetimes

The injection-level dependence of the SRH lifetime τ_{SRH} is a function of the dopant density N_A, recombination center density N_{SRH}, defect energy level E_T and capture cross sections, and for p-Si is given by:[15–17]

$$\frac{1}{\tau_{\mathrm{SRH}}}=\frac{N_A+\Delta n}{\tau_{p0}(n_1+\Delta n)+\tau_{n0}(N_A+p_1+\Delta n)}. \tag{1}$$

Here, $\Delta n=\Delta p$ is the excess carrier density, and τ_{n0} and τ_{p0} are the fundamental electron and hole lifetimes, which are related to the recombination center density, the thermal velocity[18] $v_{\mathrm{th}}=1.1\times10^{7}\,\mathrm{cm\,s}^{-1}$, and the capture cross sections via $\tau_{n0}=1/(v_{\mathrm{th}}\sigma_n N_{\mathrm{SRH}})$ and $\tau_{p0}=1/(v_{\mathrm{th}}\sigma_p N_{\mathrm{SRH}})$. The electron and hole densities when the Fermi energy coincides with the recombination center energy, n_1 and p_1, are given by:

$$n_1=N_C\exp\left(\frac{E\tau-E_C}{kT}\right), \tag{2}$$

$$p_1=N_V\exp\left(\frac{E_C-E_G-E_T}{kT}\right). \tag{3}$$

TABLE I. Energy levels and capture cross sections for Fe_i and the acceptor state of FeB pairs. Also shown are the SRH parameters n_1 and p_1, and approximations for the SRH lifetimes under low- and high-injection conditions. These approximations reveal that the FeB pair as modeled by Walz *et al.* has effectively no injection-level dependence. The low-injection approximation(*) for their level is not strictly valid for the 150 Ω cm case, but is only in error by around 20%. The parameters for Fe_i are taken from Istratov's review.[3]

Recombination center	Energy Level (eV)	σ_n (cm^{-2})	σ_p (cm^{-2})	n_1 (cm^{-3})	p_1 (cm^{-3})	Low injection τ_{SRH}	High injection τ_{SRH}
Fe_i	$E_v+0.38$	5×10^{-14}	7×10^{-17}	6.9×10^{6}	1.1×10^{13}	τ_{n0}	τ_{p0}
FeB acceptor (this work)	$E_c-0.23$	3×10^{-14}	2×10^{-15}	3.6×10^{15}	2.1×10^{4}	$\tau_{p0}(n_1/N_A)+\tau_{n0}$	τ_{p0}
FeB acceptor (Walz *et al.*)[a]	$E_c-0.29$	2.5×10^{-15}	3×10^{-14}	3.5×10^{14}	2.2×10^{5}	τ^*_{n0}	τ_{n0}

[a]See Reference 8.

Values for the effective densities of states at the conduction and valence band edges[19] are taken as $N_c=2.86\times10^{19}$ and $N_v=3.10\times10^{19}\,cm^{-3}$.

For carrier densities at which trapping effects are insignificant,[13,17] and provided the recombination center density is considerably less than the injected carrier density ($N_{SRH}\ll\Delta n$), then standard SRH theory is applicable,[17] and $\Delta n=\Delta p$ is a reasonable simplifying assumption. If one or both of these conditions are not satisfied, then the excess carrier concentrations can become strongly unequal, resulting in distorted lifetime measurements. For the majority of the data modeled in this work (the lighter iron dose of $1\times10^{11}\,cm^{-2}$), these two important conditions are easily satisfied, although for the two samples with the heavier dose of $1\times10^{12}\,cm^{-2}$ the second requirement is not strictly adhered to. The consistency of the results however, suggests that the deviations from the standard theory are small.

Under low- ($\Delta n\ll N_A$) and high-injection ($\Delta n\gg N_A$) conditions, Eq. (1) can be simplified for a given recombination center. For interstitial iron, with an energy level close to the middle of the band gap, both n_1 and p_1 are much less than N_A for all the resistivities used in this study, as shown in Table I. Hence, the right-hand side of Eq. (1) simplifies to $1/\tau_{n0}$ and $1/\tau_{p0}$ for low- and high-injection respectively, remembering that $\tau_{n0}\ll\tau_{p0}$ due to the values of the cross sections. These limiting lifetime values are independent of the dopant density, a general feature of deep levels, irrespective of their capture cross sections. However, this is not necessarily the case for the shallower acceptor state of FeB pairs. For an energy level of $E_c-0.23\,eV$, which was found to provide the best modeling results in this work, p_1 is still negligible, but $n_1\approx4\times10^{15}\,cm^{-3}$. As a result, the low-injection lifetime depends strongly on the dopant density for the resistivities used in this study. The high-injection lifetime is once again given by τ_{p0} due to the fact that $\tau_{n0}\ll\tau_{p0}$. However, the behavior of the FeB level can be entirely different if other recombination parameters are assumed. Table I also lists the energy levels and cross sections reported by Walz *et al.*, and in this case, with a slightly deeper center, $n_1\approx4\times10^{14}\,cm^{-3}$. Considering this value, and their reversed asymmetry of the cross sections, the resulting low- and high-injection lifetimes would both be approximately equal to τ_{n0}, indicating essentially no injection-level dependence, which is contrary to our experimental evidence.

Figure 2 illustrates theoretical injection-level dependent lifetime curves for three cases: interstitial iron, FeB pairs with the recombination parameters used in this work, and FeB pairs with those used by Walz. The curves, calculated for a bulk defect concentration of $1\times10^{12}\,cm^{-3}$ for each of the four resistivities used in this study, reveal the distinct behavior of each level. Note in particular the lack of injection-level dependence of Walz's parameters for the FeB pair in comparison with those used in this study. However, as mentioned, Walz only measured samples in a small range of resistivities, from 1 to 20 Ω cm, and over this narrow range the optimum parameters found in this current study also give a mild dependence with similar magnitudes (note

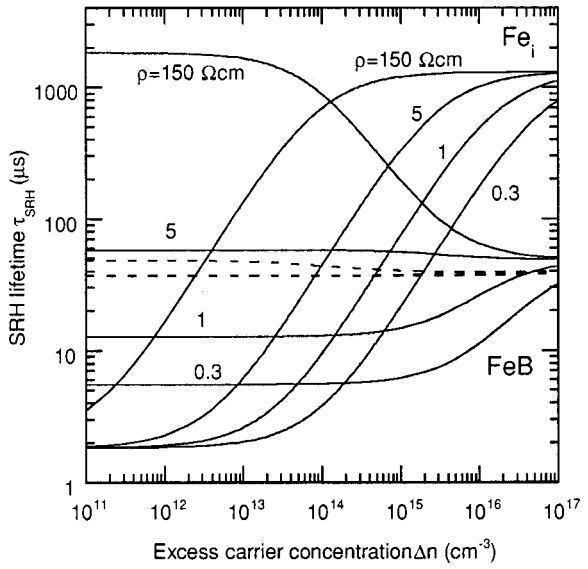

FIG. 2. SRH injection-level dependent lifetime curves for different Fe related recombination centers in *p*-type silicon of different resistivities. The density of centers has been taken as $10^{12}\,cm^{-3}$. Curves for interstitial iron (Fe_i) and the acceptor level of FeB pairs are shown for resistivities of $\rho=0.3$, 1, 5, and 150 Ω cm. The values for the energy levels and capture cross sections are given in Table I, and for FeB pairs are those determined from this study. As a comparison, curves for the acceptor level of FeB using the energy level and cross sections from Walz *et al.* (See Ref. 8) are shown for each of the four resistivities as dashed lines. The lower dashed line represents the three lower resistivities, which coincide.

the curve for the 5 Ω cm case). Hence, the parameters found in this work, and those found by Walz, provide reasonable approximations to one another over the narrower dopant range, despite the large differences between the cross section values. However, when data from a much larger dopant density range is examined, the cross sections determined in this study must be used. These considerations reveal that it is essential to have data from a large range of resistivities to *uniquely* specify the cross sections.

On a general note, Fig. 2 illustrates some interesting features of Fe/FeB pair recombination. Firstly, although the low-injection lifetime of FeB pair depends on the dopant density, these lifetimes are always significantly higher than those due to interstitial iron. Under high-injection conditions, however, the FeB pair is the dominant center. This leads to the lifetime curves for the dissociated and undissociated states for a single sample crossing over at some intermediate injection-level, which has been observed previously on several occasions.[20,21] This phenomenon highlighted the possibility of using injection-level dependent lifetimes to estimate the cross sections.

B. Modeling procedure

Lifetime measurements obtained by the QSSPC method, and by PCD methods also, represent effective lifetimes, meaning that they comprise components caused by various recombination mechanisms. It is essential therefore to be aware which mechanisms occur and what their relative contributions are in order to single out a particular mechanism for analysis. In many practical cases, more than one type of SRH center may be present simultaneously, as is the case here for iron contaminated *p*-type Si which contains both FeB pairs and Fe_i. Also, the effects of Auger recombination are often important in heavily doped or highly excited silicon,[22] and need to be considered here at the higher carrier concentrations. For reasons that will be discussed, contributions to the effective lifetime from the surfaces are not significant in the iron-diffused samples studied here, and radiative recombination is negligible in indirect semiconductors such as silicon. Therefore, the effective lifetime, comprising all of the important contributions, can be expressed as:

$$\frac{1}{\tau_{\text{eff}}} = \frac{1}{\tau_{\text{SRH}}^{\text{Fe}}} + \frac{1}{\tau_{\text{SRH}}^{\text{FeB}}} + \frac{1}{\tau_{\text{Auger}}}, \tag{4}$$

The Auger lifetime is calculated using a Coulomb-enhanced Auger recombination model[23,24] which is valid for all injection-levels and dopant densities. Values for the Auger coefficients C_n, C_p, and C_a, as required in the Auger model, are taken from the literature.[22,25]

The fitting procedure employed in this work essentially proceeds as follows. Curves such as those in Fig. 2 are taken for interstitial iron and FeB pairs for the appropriate resistivity. These curves are combined in a linear fashion according to Eq. (4), with a term for Auger recombination included, and compared to the measured data. The concentrations of each center are adjusted, and the shape of the FeB curve altered by changing the cross sections, until a good fit is obtained for all the samples with a single set of cross sections. It so happens that the less heavily doped samples yield data which is more sensitive to the value of σ_n, while the more heavily doped data allows accurate determination of σ_p.

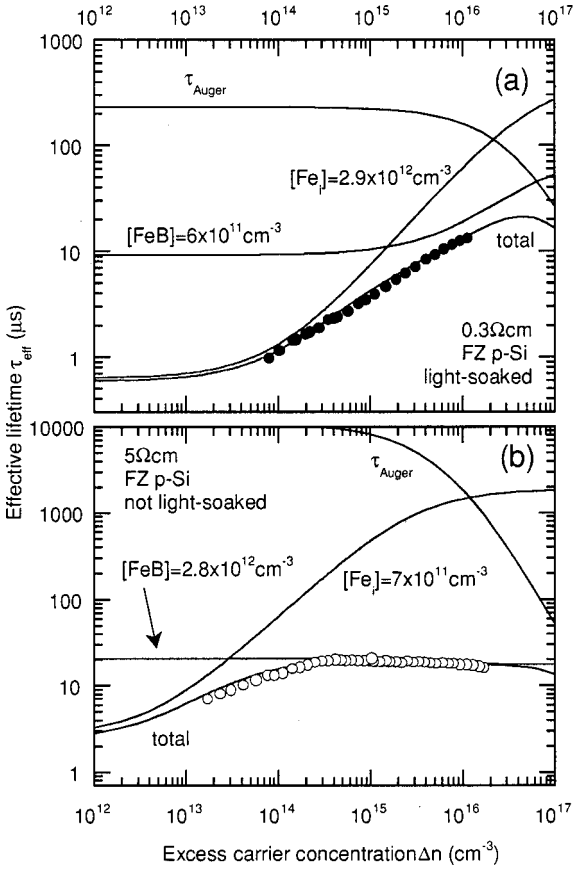

FIG. 3. Examples of the fitting procedure for the effective lifetimes for: (a) the 0.3 Ω cm sample with light soaking, and (b) the 5 Ω cm sample without light soaking. The constituent curves for Fe_i, FeB pairs, and Auger recombination are shown for each plot, and the concentrations of the recombination centers used for the fits are given in Table II. In both cases, the implanted dose was $1\times10^{11}\,\text{cm}^{-2}$.

Two examples of the fitting process are given in Fig. 3. in Fig. 3(a), the light-soaked case for the 0.3 Ω cm sample is shown. Due to the light soaking, the majority of the iron present in this sample occurs as interstitial iron. In Fig. 3(b) data for the 5 Ω cm sample without light soaking is shown, and is dominated by the presence of FeB pairs. Note that the dependence of the FeB pair curves is markedly different for the two resistivities, while the shape of the Fe_i curves are similar apart from being shifted due to the change in dopant density. It is an interesting coincidence that the linear combination of the FeB and Fe_i terms gives rise to a straight line in Fig. 3(a).

For all samples, the sum of the modeled interstitial iron and FeB pair concentrations is forced to agree with that expected from the implantation dose. For Figs. 3(a) and 3(b), this sum equals $3.5\times10^{12}\,\text{cm}^{-3}$, precisely that expected from an implant dose of $1\times10^{11}\,\text{cm}^{-2}$ in a wafer of thickness 0.0285 cm. This process effectively determines the concentration of FeB pairs for any curve, leaving the two cross sections of the FeB pairs as the only free parameters in the procedure. In principle, therefore, only two largely different

TABLE II. Modeled and implanted iron concentrations for the different resistivity samples under different light-soaking conditions. Note that the sum of the modeled Fe_i and FeB pair concentrations is always close to the total iron concentration expected from the implantation dose. Under strong lightsoaking most of the iron is present as Fe_i, whereas without light-soaking FeB pairs dominate.

Resistivity (Ω cm)	N_A (cm^3)	W (cm)	Fe implant dose (cm^{-2})	[Fe] (cm^{-3}) from dose	Light soaking	Modeled [Fe_i] (cm^{-3})	Modeled [FeB] (cm^{-3})	[Fe_i]+[FeB]
0.3	6.6×10^{16}	0.0285	1.0×10^{11}	3.5×10^{12}	none	1.0×10^{12}	2.5×10^{12}	3.5×10^{12}
,,	,,	,,	,,	,,	partial	2.0×10^{12}	1.5×10^{12}	,,
,,	,,	,,	,,	,,	full	2.9×10^{12}	0.6×10^{12}	,,
1	1.7×10^{16}	0.0400	1.0×10^{11}	2.5×10^{12}	none	0.2×10^{12}	2.3×10^{12}	2.5×10^{12}
,,	,,	,,	,,	,,	partial	1.1×10^{12}	1.4×10^{12}	,,
,,	,,	,,	,,	,,	full	2.0×10^{12}	0.5×10^{12}	,,
,,	,,	,,	1.0×10^{12}	2.5×10^{13}	none	0.2×10^{13}	2.0×10^{13}	2.2×10^{13}
5	3.0×10^{15}	0.029	1.0×10^{11}	3.5×10^{12}	none	0.7×10^{12}	2.8×10^{12}	3.5×10^{12}
,,	,,	,,	,,	,,	full	3.2×10^{12}	0.3×10^{12}	,,
150	9×10^{13}	0.035	1.0×10^{12}	2.9×10^{13}	none	0.5×10^{13}	2.0×10^{13}	2.5×10^{13}

resistivities are needed to obtain unique values of the cross sections. However, the fact that these values also generate good results for the other resistivities used in this study, and also for the different concentrations of FeB pairs as brought about by light soaking, provides greater confidence in the validity of the underlying method.

V. RESULTS AND DISCUSSION

Figure 1 depicts the results for the 1 Ω cm samples. The Auger lifetime represents an intrinsic upper limit in *p*-type silicon samples of this resistivity, which is approached by the control sample. Below these curves are data for two iron implanted samples, with doses of 1×10^{11} and $1\times10^{12}\,cm^{-2}$. There are three curves for the lighter dose corresponding to different light-soaking levels, and hence different relative populations of Fe_i and FeB pairs. The solid lines which pass through the data represent the SRH lifetimes as calculated using the appropriate recombination parameters for FeB and Fe_i as given in Table I. Table II lists the concentrations of Fe_i and FeB pairs that were used to obtain the fits. The fact that these concentrations add to agree with that expected from the dose indicates that very little precipitation has occurred in the samples. This is further corroborated by the fact that a good fit for the heavier dose can be achieved by merely scaling up the concentrations by an order of magnitude (see Table II), as should occur if precipitation is negligible. It is interesting to note that even in the fully light-soaked case, it is still necessary to include a small number of FeB pairs to describe the data well, indicating that either pair dissociation is not complete or that some repairing occurs between light soaking and lifetime measurement.

Figures 4 and 5 show the results for the 0.3 and 5 Ω cm samples, respectively, both implanted with a dose of $1\times10^{11}\,cm^{-2}$, under different light-soaking conditions. Once again, the sum of the modeled concentrations agrees well with that obtained from the dose. Note that the lifetimes of the control samples approach the Auger limit much more closely for the 0.3 Ω cm case, indicating that these wafers are of better intrinsic quality. An important observation here is that the dependence of the two resistivities without light soaking goes in opposite directions as the carrier density increases, as expected from Fig. 2. The change in dependence is only mild however, reflecting the fact that the dopant densities for these two cases are not too far removed from the value of n_1.

For the 150 Ω cm light-soaked case however, the dependence becomes much more pronounced, as revealed by the data and fit in Fig. 6. In this plot, the constituent SRH curves for the FeB pairs and Fe_i are also shown, similar to Fig. 3. The strong dependence of the FeB curve is clear in this case, which contrasts with the weak dependence predicted by Walz's cross sections (see Fig. 2). This comment also holds for the other extreme of dopant densities as shown in Fig. 4 for the 0.3 Ω cm case, with the notable difference that the injection-level dependence goes in the opposite direction. The data in Fig. 6 is for a sample that was implanted with a heavier dose of $1\times10^{12}\,cm^{-2}$. For this resistivity, the corresponding wafer with the lighter dose gave lifetime data that was too close to the control sample, meaning that surface recombination impacted on the measurements.

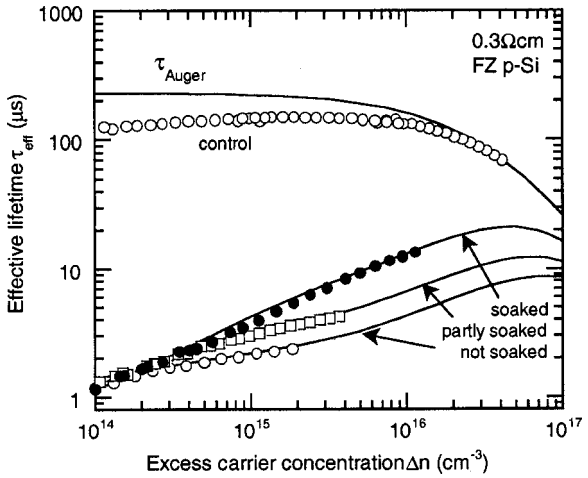

FIG. 4. Lifetime measurements (symbols) and SRH fits (solid lines) for the 0.3 Ω cm sample implanted with an iron dose of $1\times10^{11}\,cm^{-2}$. Three curves corresponding to different light soaking levels are shown. The concentrations of Fe_i and FeB pairs used to generate the fits are given in Table II, and the recombination parameters in Table I.

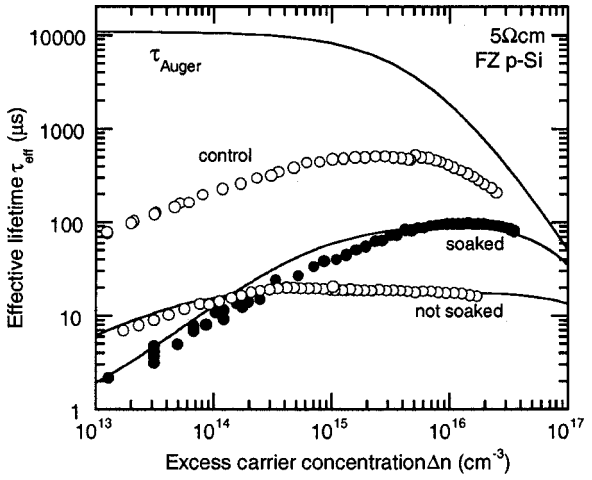

FIG. 5. Lifetime measurements (symbols) and SRH fits (solid lines) for the 5 Ω cm sample implanted with an iron dose of $1\times10^{11}\,\mathrm{cm}^{-2}$. Two curves corresponding to different light soaking levels are shown. The concentrations of Fe_i and FeB pairs used to generate the fits are given in Table II, and the recombination parameters in Table I.

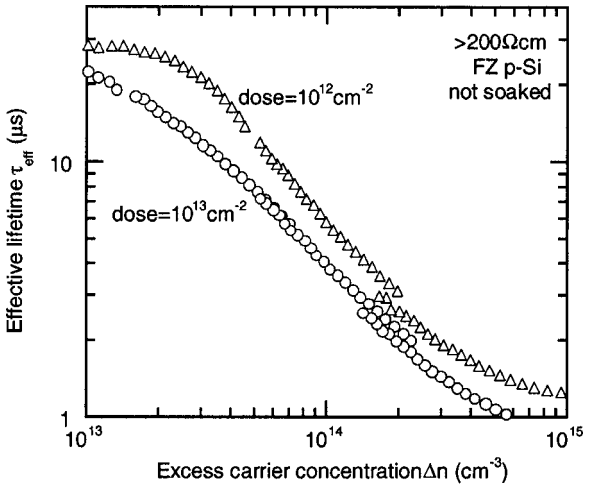

FIG. 7. Lifetime measurements for high resistivity (>200 Ω cm) samples implanted with iron doses of $1\times10^{12}\,\mathrm{cm}^{-2}$ and $1\times10^{13}\,\mathrm{cm}^{-2}$. The small difference in recombination lifetimes reflects precipitation of iron during annealing.

For all of the fits shown, the capture cross sections used for the FeB pairs were $\sigma_n=3\times10^{-14}\,\mathrm{cm}^{-2}$ and $\sigma_p=2\times10^{-15}\,\mathrm{cm}^{-2}$. It is possible to estimate the uncertainty in these values by adjusting them and observing the effect on the fits. As mentioned, the more heavily doped samples are more sensitive to the electron capture cross section, while the high resistivity samples are more strongly affected by the hole cross section. In conjunction with a typical uncertainty in the measured lifetimes of around 20%, and an uncertainty of about 5% in the dopant densities, we can state that the cross sections should reside in the ranges $\sigma_n=(3\pm2)\times10^{-14}\,\mathrm{cm}^{-2}$ and $\sigma_p=(2\pm1)\times10^{-15}\,\mathrm{cm}^{-2}$. The value of the energy level used was $E_c-0.23\,\mathrm{eV}$, which is somewhat different to that found in some studies,[5,6,8] but nevertheless within the uncertainty bounds reported by Istratov in his recent review of iron complexes in silicon.[3] It should be mentioned that our finding that $\sigma_n>\sigma_p$ is contradictory to the results of Walz, and also to expectations based on Coulombic effects due to the charge state of the acceptor level (FeB). However, cross sections are not only determined by the charge state, but also by the energy level, hence it is possible that the proximity of the FeB acceptor level to the conduction band may negate the Coulombic repulsion for electrons.

Note that for both the heavier doses of $1\times10^{12}\,\mathrm{cm}^{-2}$ (Figs. 1 and 6), the sum of the modeled iron-related centers is a little less than expected, as shown in Table II. This is possibly due to a small amount of precipitation, since these doses are close to the solubility limit for the 900 °C anneal. In fact, the concentrations reported in Table II suggest that around 10% of the iron has precipitated, in accordance with the expectations from Henley's data,[11] as previously discussed.

Figure 7 illustrates the problems that can arise from severe precipitation as a result of inappropriate sample preparation. These high resistivity wafers (>200 Ω cm) were implanted with iron doses of $1\times10^{12}\,\mathrm{cm}^{-2}$ and $1\times10^{13}\,\mathrm{cm}^{-2}$ and annealed at 900 °C. If all of the available iron was distributed uniformly throughout the bulk, these doses would correspond to bulk concentrations of $3.3\times10^{13}\,\mathrm{cm}^{-3}$ and $3.3\times10^{14}\,\mathrm{cm}^{-3}$, respectively. However, as mentioned, the solubility limit of interstitial iron at 900 °C is around $5\times10^{13}\,\mathrm{cm}^{-3}$. Consequently, the more heavily implanted ($1\times10^{13}\mathrm{Fe\,cm}^{-2}$) sample will be subject to considerable loss of iron through precipitation, in fact about 85% will precipitate according to the solubility value. Figure 7 shows that this has indeed occurred, as evidenced by the small difference in the magnitudes of the recombination lifetimes for the two samples. If there had been no precipitation, doses which differed by an order of magnitude should have resulted in lifetimes that differed by the same factor, as occurred for the two doses in Fig. 1 (within 10%). However, the lifetimes for the two doses in Fig. 7 differ by at most a factor of two (when compared at the same injection level), implying that at

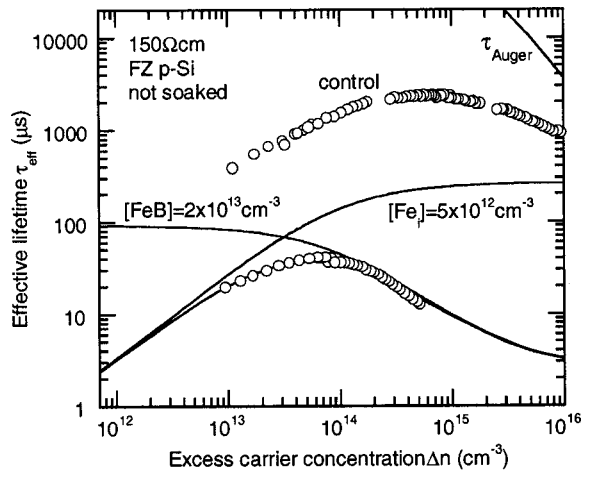

FIG. 6. Lifetime measurements (symbols) and SRH fit (solid lines) for the 150 Ω cm sample implanted with an iron dose of $1\times10^{12}\,\mathrm{cm}^{-2}$. The curve shown is for no light soaking. The concentrations of Fe_i and FeB pairs used to generate the fit are given in Table II, and the recombination parameters in Table I.

least 80% of the iron has precipitated in the heavier dose (1×10^{13}Fe cm^{-2}), in agreement with expectations from the solubility data.

Precipitation was one reason for leaving the data for the heavily implanted sample in Fig. 7 out of the modeling exercise. However, both these wafers suffer from other problems and as a result both sets of data were excluded. For both samples, the recombination center density is comparable to or greater than both the dopant density ($N_A<6\times10^{13}\,\mathrm{cm}^{-3}$) and also the carrier densities at which the lifetime is to be measured. This implies that the excess carrier populations can become heavily unequal due to ''trapping'' by the recombination centers, particularly if the capture cross sections are largely different. These effects can significantly distort the lifetime data, making standard SRH modeling inappropriate. Nevertheless, the general trend in Fig. 7 agrees with the theoretical expectations indicated in Fig. 2, considering that the lifetime is shifted to much lower values due to the higher iron concentration in the sample in Fig. 7.

Up to this point, we have only considered FeB acceptors, and the shallower donor level has not been included in the modeling. But, curiously, it is also possible to obtain satisfactory fits to all samples, with an energy level of $E_v+0.1\,\mathrm{eV}$ and capture cross sections of $\sigma_n=3\times10^{-13}\,\mathrm{cm}^{-2}$ and $\sigma_p=3\times10^{-15}\,\mathrm{cm}^{-2}$, plus the level for interstitial iron. This apparent weakness in the method, that is, its inability to identify the level causing the recombination, arises because of the indiscriminate treatment of the cross sections and the energy levels in the standard SRH statistics. It is necessary to invoke a physical argument, such as Brotherton[5] did, as mentioned in the Introduction, to decide which center is dominant. The fact that neither the acceptor nor the donor FeB center are deep, means that the low-injection lifetime may vary with the dopant density, depending on the values of p_1 and n_1. This is the important criterion for describing the changing injection-level dependence for the different resistivities as revealed by our data. However, although the method can not discriminate between these two levels, it is able to do so for the acceptor levels at $E_c-0.23$ and $E_c-0.29\,\mathrm{eV}$, indicating that the ''degeneracy'' of the $E_v+0.1$ and $E_c-0.23\,\mathrm{eV}$ levels is somewhat coincidental.

VI. CONCLUSIONS

SRH recombination statistics have been fitted to experimental data from *p*-type silicon samples contaminated with known doses of iron. By using a large range of dopant densities, the changing injection-level behavior of the acceptor level of FeB pairs allows accurate determination of the electron and hole capture cross sections for this level at room temperature. The best fits across all samples were obtained with values of $E_c-0.23\,\mathrm{eV}$ for the energy level, and $\sigma_n=3\times10^{-14}\,\mathrm{cm}^{-2}$ and $\sigma_p=2\times10^{-15}\,\mathrm{cm}^{-2}$ for the electron and hole capture cross sections, respectively. More generally, this work illustrates that with appropriate choices of implant dose, annealing temperature and time, and a good range of substrate resistivities, injection-level spectroscopy offers an accurate alternative to DLTS techniques for determining capture cross sections of defects in semiconductors, especially if the defect energy is known.

ACKNOWLEDGMENTS

The authors are grateful to Mark Kerr and C. Jagadish of the ANU for helpful discussions, and also to Mark Kerr for depositing the SiN films. This work has been supported by the Australian Research Council (ARC). One of the authors (J.W.L.) is also grateful to the ARC for funding under the fellowship program.

[1] G. Zoth and W. Bergholz, J. Appl. Phys. **67**, 6764 (1990).
[2] J. Lagowski, P. Edelman, A. M. Kontkiewicz, O. Milic, W. Henley, M. Dexter, L. Jastrzebski, and A. M. Hoff, Appl. Phys. Lett. **63**, 3043 (1993).
[3] A. A. Istratov, H. Hieslmair, and E. R. Weber, Appl. Phys. A: Mater. Sci. Process. **69**, 13 (1999).
[4] J. Schmidt and A. Cuevas, J. Appl. Phys. **86**, 3175 (1999).
[5] S. D. Brotherton, P. Bradley, and A. Gill, J. Appl. Phys. **57**, 1941 (1985).
[6] Y. Hayamizu, T. Hamaguchi, S. Ushio, and T. Abe, J. Appl. Phys. **69**, 3077 (1991).
[7] A. Kaniava, E. Gaubas, J. Vaitkus, J. Vanhellemont, and A. L. P. Rotondaro, Mater. Sci. Technol. **11**, 670 (1995).
[8] D. Walz, J.-P. Joly, and G. Kamarinos, Appl. Phys. A: Mater. Sci. Process. **62**, 435 (1996).
[9] J. Wong-Leung, D. J. Eaglesham, J. Sapjeta, D. C. Jacobson, J. M. Poate, and J. S. Williams, J. Appl. Phys. **83**, 580 (1998).
[10] J. Schmidt and M. Kerr, Sol. Energy Mater. Sol. Cells **65**, 585 (2001).
[11] W. B. Henley and D. A. Ramappa, J. Appl. Phys. **82**, 589 (1997).
[12] R. A. Sinton and A. Cuevas, Appl. Phys. Lett. **69**, 2510 (1996).
[13] D. Macdonald and A. Cuevas, Appl. Phys. Lett. **74**, 1710 (1999).
[14] H. Hashizume, S. Sumie, and Y. Nakai, in *Recombination Lifetime Measurements in Silicon*, ASTM STP 1340, edited by D. C. Gupta, F. R. Bacher, and W. M. Hughes (American Society for Testing Materials, Philadelphia, 1998).
[15] W. Shockley and W. T. Read, Phys. Rev. **87**, 835 (1952).
[16] R. N. Hall, Phys. Rev. **87**, 387 (1952).
[17] J. S. Blakemore, *Semiconductor Statistics*, International Series of Monographs on Semiconductors, Vol. 3 (Pergamon, Oxford, 1962).
[18] W. M. Bullis and H. R. Huff, J. Electrochem. Soc. **143**, 1399 (1996).
[19] M. A. Green, J. Appl. Phys. **67**, 2944 (1990).
[20] R. Falster and G. Barionetti, in *Recombination Lifetime Measurements in Silicon*, ASTM STP 1340, edited by D. C. Gupta, F. R. Bacher, and W. M. Hughes (American Society for Testing Materials, Philadelphia, 1998).
[21] G. Zoth, in *Recombination Lifetime Measurements in Silicon*, ASTM STP 1340, edited by D. C. Gupta, F. R. Bacher and W. M. Hughes (American Society for Testing Materials, Philadelphia, 1998).
[22] J. Dziewior and W. Schmid, Appl. Phys. Lett. **31**, 346 (1977).
[23] P. P. Altermatt, J. Schmidt, G. Heiser, and A. G. Aberle, J. Appl. Phys. **82**, 4938 (1997).
[24] S. W. Glunz, D. Biro, S. Rein, and W. Warta, J. Appl. Phys. **86**, 683 (1999).
[25] R. A. Sinton and R. M. Swanson, IEEE Trans. Electron Devices **34**, 1380 (1987).